Electronic Supplementary Information

Self-assembly to synchrony of active gels

Pawan Kumar[a], Dezső Horváth[b], Ágota Tóth[a*]
[a]Department of Physical Chemistry and Materials Science, University of Szeged, Rerrich Béla tér 1., Szeged, H-6720, Hungary.
[b]Department of Applied and Environmental Chemistry, University of Szeged, Rerrich Béla tér 1., Szeged, H-6720, Hungary.

CONTENTS

Modeling S2

Supporting figures S3

Supporting videos S10

References S10

CS(sol) w/V %	CS(CE) w/V%	CS(CGE) w/V%	CS(CG) w/V%	CS w/V%	ρ (g/cm^3)	η (mPa.s)	γ (mN/m)	m (mg)
0.75	–	0.647	–	–	1.0047	46.24	46	30.9
0.75	–	–	0.647	–	1.0218	32.70	62	44.8
0.75	–	–	–	0.647	1.0010	71.49	59	44.5
1.5	1.293	–	–	–	0.9859	639.7	–	32.3
1.5	–	1.293	–	–	1.0066	371.2	–	32.3
1.5	–	–	–	1.293	1.0033	455.6	–	45.0

Table S1: Densities (ρ) and dynamic viscosities (η) of the reactants chitosan-ethanol (CE), chitosan-gadolinium-ethanol (CGE), chitosan-gadolinium (CG) and chitosan (CS) for the CS(sol) concentrations of 0.75 w/V % and 1.5 w/V %. The mass of a droplet (m) dripped with a plastic needle with an inner diameter of 1.65 mm.

MODELING

To solve the ordinary differential equations in Eqn. (3) with Eqn. (4) in the manuscript, the CVODE [1] solver with the Backwards Differentiation Formula (BDF) is used from the SUNDIALS [2] package with relative tolerances of 10^{-8}, and absolute tolerances of 10^{-12}.

The dimensionless parameters were set to $\beta = 4.2$, $k = 3.5$, with $\alpha' = 2.47$ and $q' = 2.1$ in Eqn. (4). The damping coefficient C in Eqn. (3) is set to 0.006.

SUPPORTING FIGURES

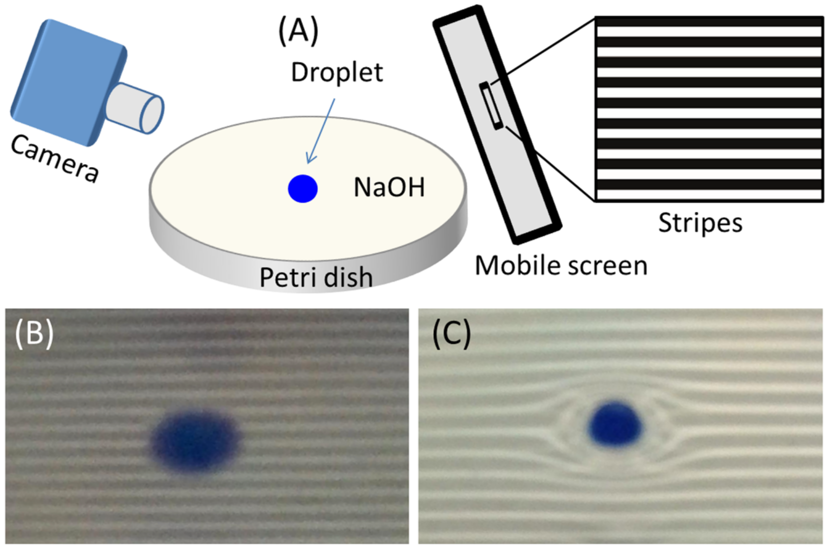

Figure S1: (A) Schematic setup to determine the deformation of the alkaline solution at the air-liquid interface by placing CS and CG droplets. The camera was positioned incline to the Petri dish to capture the reflection of stripe pattern. The parallel lines of stripe pattern near the locality of (B) CS gel indicate the flat surface of NaOH solution, and (C) the diverging lines around the CG droplet show concave deformation. The CS(sol) concentrations is (B) 1.5 % w/V and (C) 0.75 % w/V, and d_i =11.65 mm.

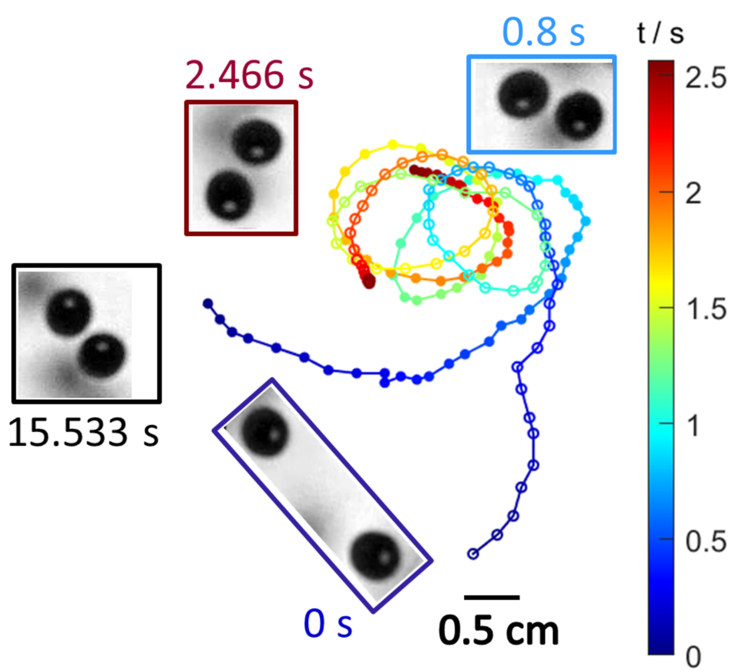

Figure S2: The representative color trajectories of two beads. Images in the figure indicate the beads' position at t=0, t=0.8 s, t=2.466 s, and t=15.533 s. They show that beads form a pair and propel in a group after the collision.

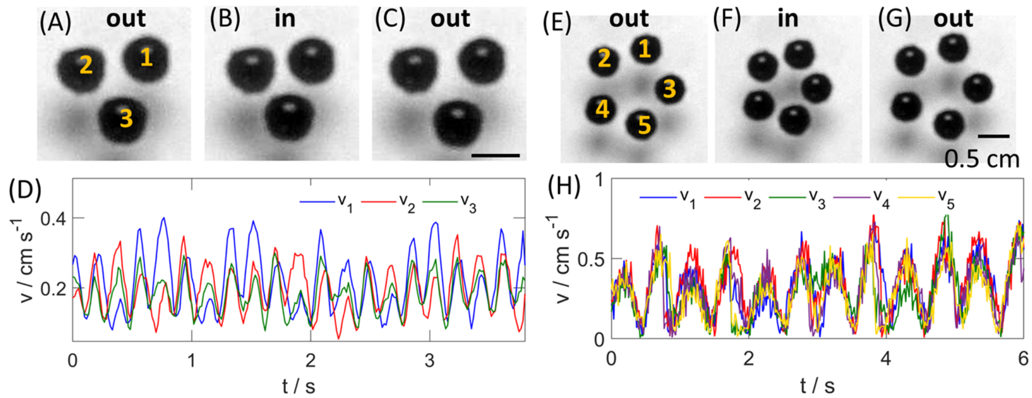

Figure S3: Clustering of three (A-D) and five (E-H) beads indicating the (A, C) and (E, G) breathing-out, and (B) and (F) breathing-in modes, respectively. The speed evolution of three and five beads in (D) and (H) shows their synchronous behavior. CS(sol) = 0.75 % w/V and d_i = 1.65 mm.

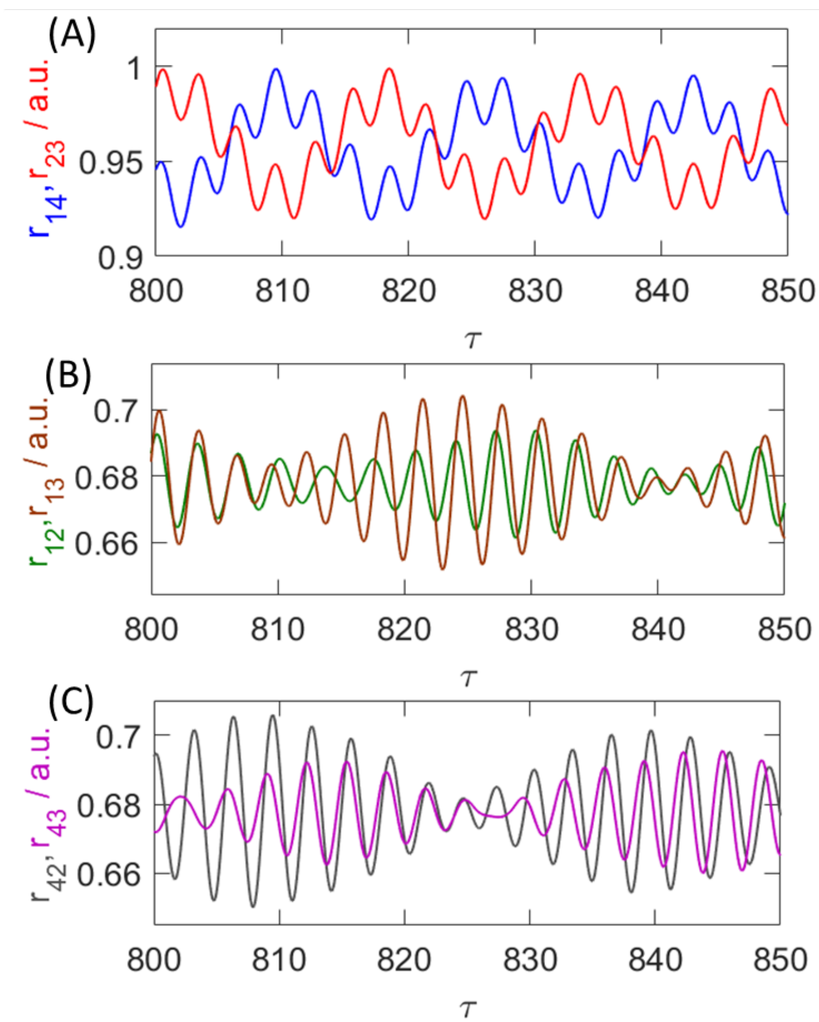

Figure S4: Dynamics of radial distances between particles with their initial positions (0, 0), (0.8, 0.8), (0.4, -0.4) and (0.8, 0.0). (A) Synchronized state between particles (1,4) and (2,3). (B-C) The phase drifting in the time series shows unsynchronized behavior.

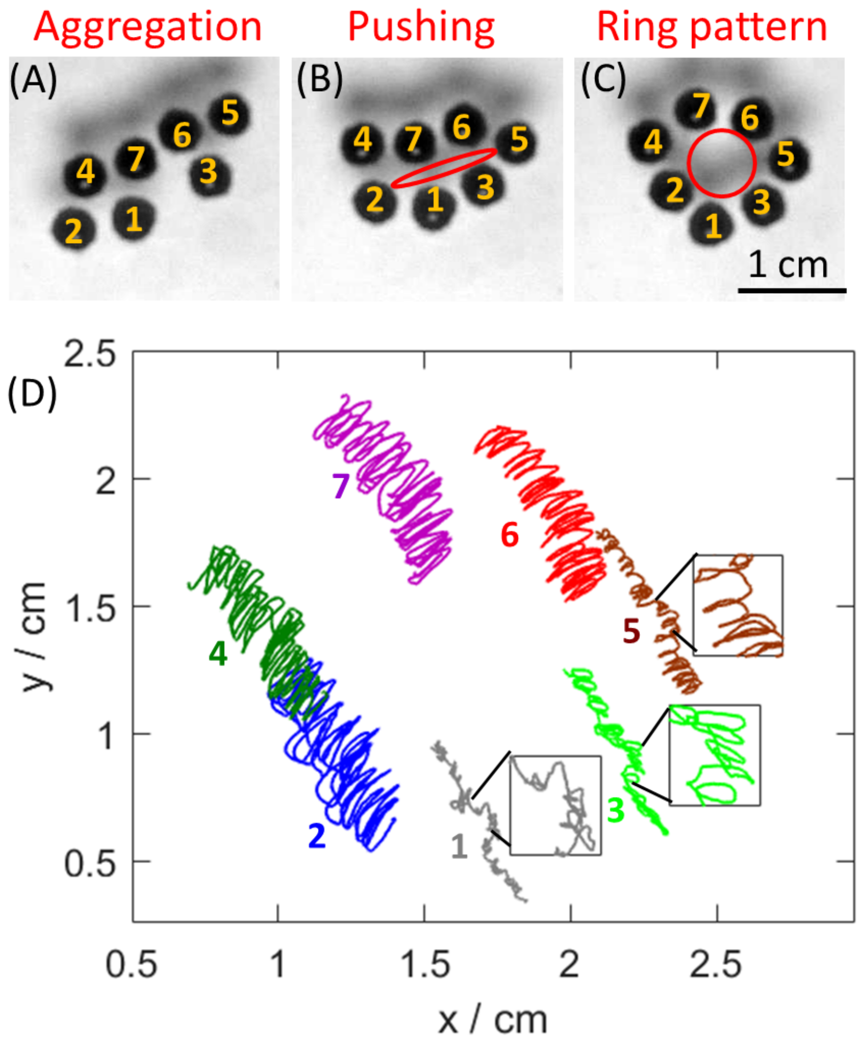

Figure S5: When beads (A) aggregate due to capillary interaction, the chemical gradients (B) push them away and create (C) a ring pattern. (E) Bead trajectories in the $x-y$ plane. The circular loops for beads 2–7 show oscillatory motion. Bead 1 does not exhibit significant oscillations, but the change in position occurs because of the collective propulsion of the assembly. CS(sol) = 0.75 % w/V and d_i = 1.65 mm.

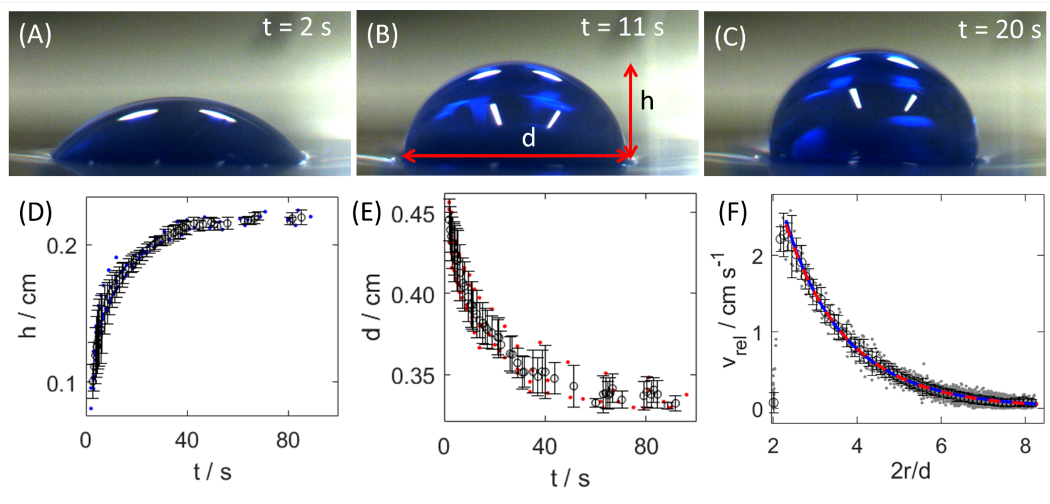

Figure S6: (A-C) Images represent the evolution of CG droplet on the air-liquid interface. Field of view: 0.64 × 0.31 cm^2. Growth of (D) height h and (E) diameter d of the droplet in the upper region with time. The black error bars display the binned data of the five separate experiments. (F) Relative velocity of the CG beads as a function of the ratio of distance from their centroid and bead radius. The red dashed curve corresponds to the fitting of equation $v_{rel} = \frac{G_F}{\sqrt{2r/d}} G(2r/d) \exp(-qr)$ with parameters q = 2.27 ± 0.10 cm^{-1} and G_F = 15.19 ± 2.00 cm s^{-1} and blue curve fits with parameters q = 2.16 ± 0.10 and G_F =12.32± 1.53 cm s^{-1} when G(2r/d) =1. The concentration of CS(sol) is used 1.5 % w/V and d_i is 1.65 mm.

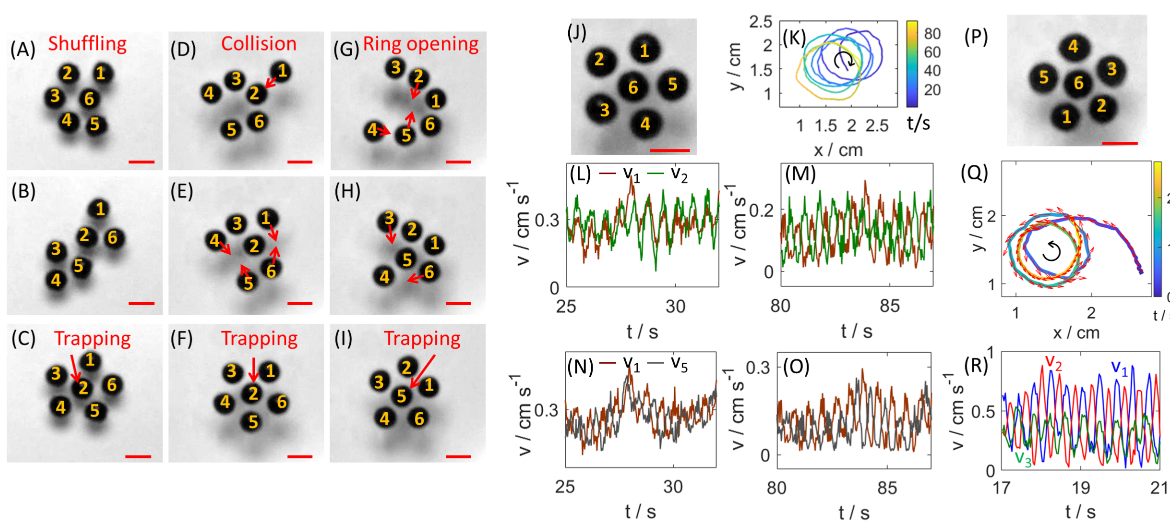

Figure S7: Shuffling of the beads (A-B) induces traping (C). The collision of bead 1 to 2 (D) pushes bead 2 inside (E) and creates a star pattern (F). As the ring opens, bead 4 leaves contact with 5 (G), further bead 5 moves in, and 4 towards bead 5 (H) and bead 5 traps (I). The arrows in (D, E) and (G, H) indicate the direction of beads' motion. (J) Star pattern and (K) clockwise rotational trajectory of bead 2. Speed dynamics of beads 1 and 2 (L) in-phase and (M) anti-phase. In the case of beads 1 and 5 (N-O), the speed remains near anti-phase synchrony when they oscillate. The formation of (P) star pattern, (Q) rotates in anti-clockwise direction (bead 1 $x-y$ trajectory). (R) Relay synchrony of beads, where (1,3) in-phase and (1,2) anti-phase. CS(sol) = 1.5 % w/V and d_i is 1.65 mm. Scale bar = 0.5 cm.

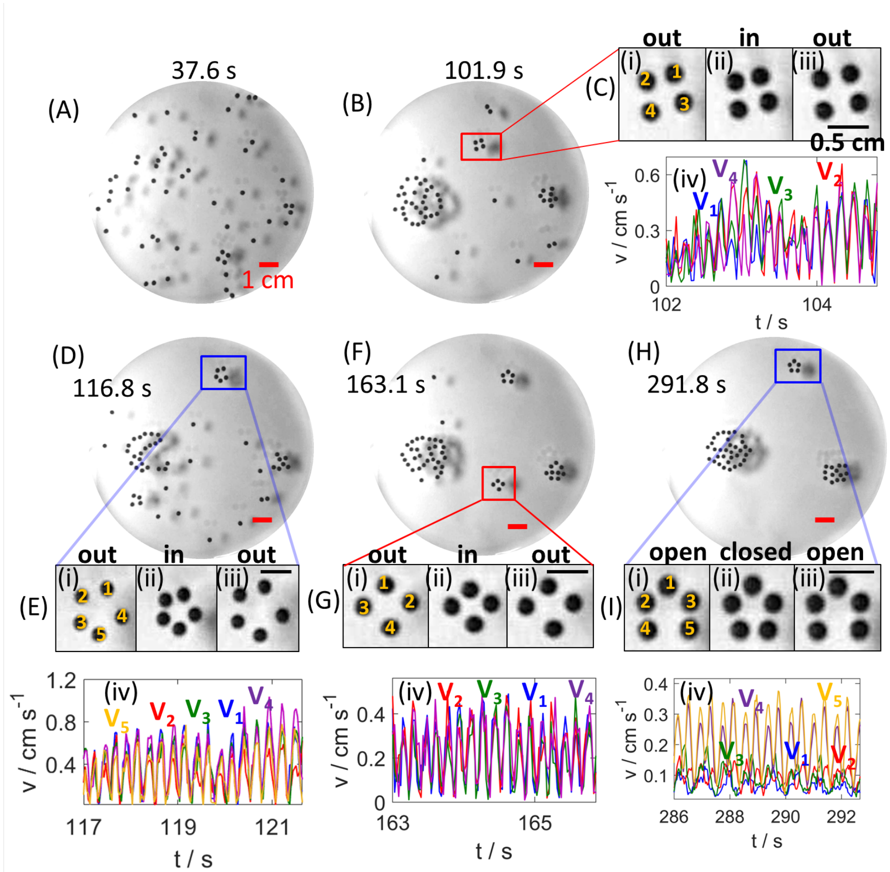

Figure S8: (A) Smaller groups form and disperse away. (B) Multiple clusters appear, where the (C) aggregation of four beads oscillates (i, iii) breathing-out, (ii) breathing-in states with an average time-period of 0.32 $\pm$ 0.02 s, and (iv) speed dynamics indicates the collective oscillations in synchrony. (D) Interaction of nearest bead with four beads transforms into a cluster of five (E), which exhibits (i, iii) breathing-out, (ii) breathing-in modes in (iv) synchrony with time-period of 0.5 $\pm$ 0.03 s. (F, G) Another cluster of four beads synchronously breathing-out and -in with time-period of 0.39 $\pm$ 0.02 s. (H) In the later stage, the ring pattern of (I) five beads (i, iii) open and (ii) closed together with time-period of 0.8 $\pm$ 0.2 s. (iv) The speed dynamics show the partial synchrony of the beads. The CS(sol) concentration is 1.5 % w/V and d_i = 0.6 mm.

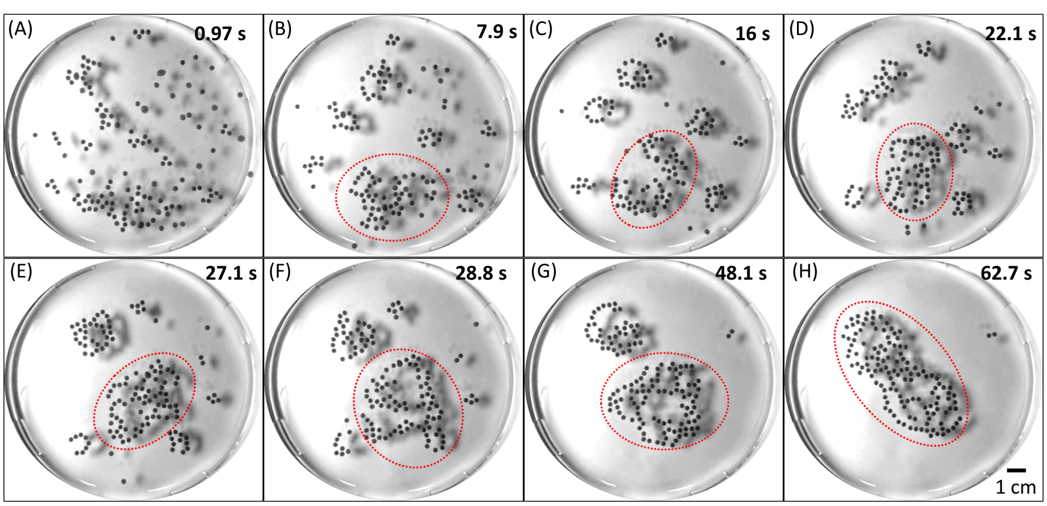

Figure S9: Clustering of beads with time. (A-C) Multiple clusters with 54 (B) and 56 (C) beads, (D-F) smaller groups merge into the larger clusters with 55 (D), 67 (E), and 79 (F) beads, (G) two large groups with 90 and 39 beads merge into (H) a single large cluster with 129 beads. The red dotted circles guide the formation bigger cluster. Time t=0 is considered when the last CGE droplet is placed in the alkaline solution. CS(sol) = 1.5 % w/V and d_i = 0.6 mm.

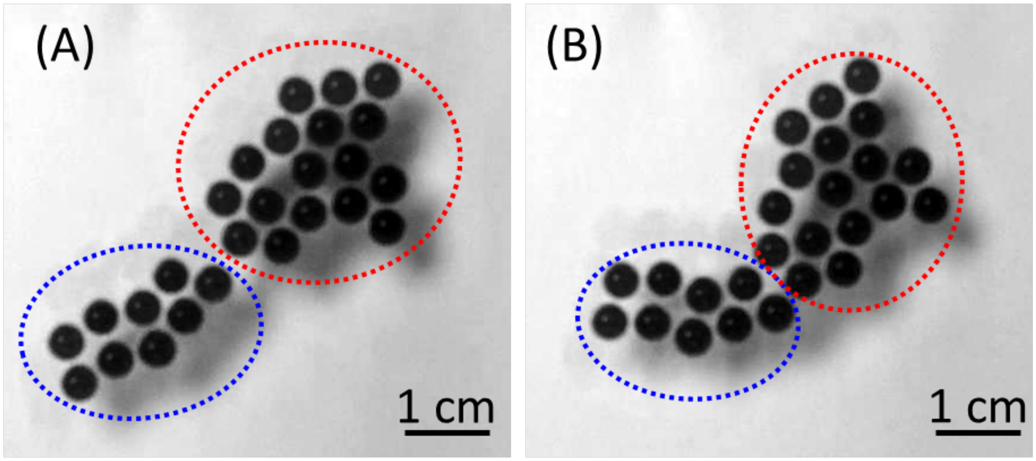

Figure S10: Interaction of two passive groups of CG droplets (A) before (D) after the collision. The blue and red dots guide the eye to visualize the two groups, which remain static after the collision. The CS(sol) concentration is 0.75 % w/V and d_i = 1.65 mm.

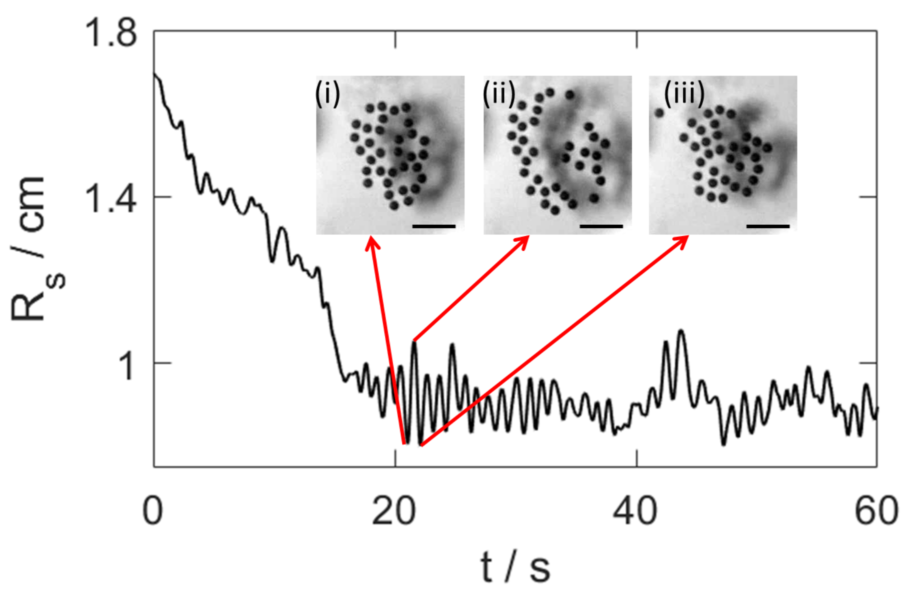

Figure S11: Swarm radii of a group of 33 CGE particles. The swarming of the active particles exhibits oscillatory motion. The inset images (i, iii) are the close packing of the particles (shrinkage state), and (ii) is the expansion state. Scale bar = 1 cm. CS(sol) = 1.5 % w/V and d_i = 0.6 mm.

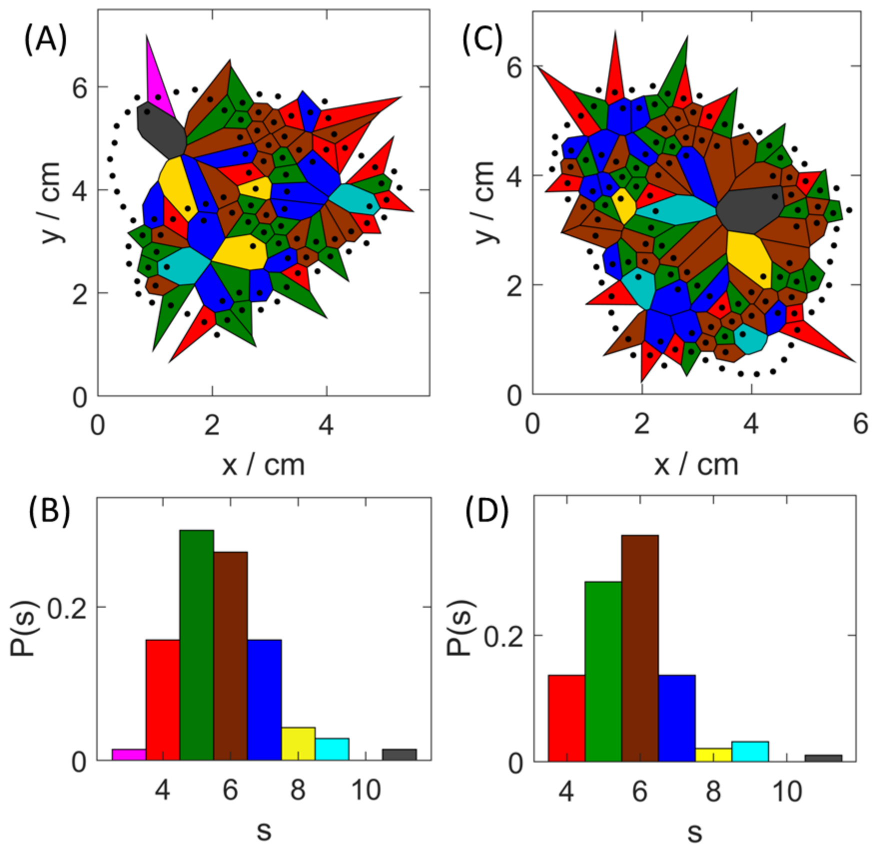

Figure S12: (A,C) Voronoi diagrams and (B, D) their associated distribution histograms of number of neighboring beads s for (A, B) 99 and (C, D) 129 beads. CS(sol) concentration is 1.5 % w/V, and d_i = 0.6 mm.

SUPPORTING VIDEOS

Movie S1: Collective synchronization of breathing mode of four CGE beads for the concentration of CS(sol) 0.75 w/V % with $d_i = 1.65$ mm, shown at 3X the actual speed. Field of view: 2.46×2.36 cm^2.

Movie S2: Collective synchronization of breathing mode of four active particles based on Eqns (3-4).

Movie S3: Synchronization of chain pattern with different amplitudes of groups, shown at 3X the actual speed. The concentration of CS(sol) is 0.75 w/V % and $d_i = 1.65$ mm. Field of view: 2.80×2.59 cm^2.

Movie S4: Oscillating ring pattern for the concentration of CS(sol) 0.75 w/V % with $d_i = 1.65$ mm, shown at 5X the actual speed. Field of view: 2.93×3.19 cm^2.

Movie S5: Cluster synchronization of gel beads for the concentration of CS(sol) 1.5 w/V % with $d_i = 1.65$ mm, shown at 4X the actual speed. Field of view: 2.72×2.97 cm^2

Movie S6: Oscillating rotor in relay synchrony, shown at 8X the actual speed. The concentration of CS(sol) is 1.5 w/V % and $d_i = 1.65$ mm. Field of view: 4.00×3.29 cm^2

Movie S7: Disk formation and swarming of a large cluster for the concentration of CS(sol) 1.5 w/V % and $d_i = 0.6$ mm, shown at 6X the actual speed. Field of view: 10.15×9.78 cm^2.

[1] S. D. Cohen, A. C. Hindmarsh, and P. F. Dubois, Computers in Physics **10**, 138 (1996).
[2] A. C. Hindmarsh, P. N. Brown, K. E. Grant, S. L. Lee, R. Serban, D. E. Shumaker, and C. S. Woodward, ACM Trans. Math. Softw. **31**, 363 (2005).